CHEMICAL ENGINEERING TRANSACTIONS
VOL. 57, 2017
A publication of AIDIC
The Italian Association of Chemical Engineering
Online at www.aidic.it/cet
Guest Editors: Sauro Pierucci, Jiří Jaromír Klemeš, Laura Piazza, Serafim Bakalis

ISBN 978-88-95608- 48-8; **ISSN** 2283-9216

Analysis of Mechanical Behavior of a Device Made of Poly L Lactide Acid for Reconstruction of Phalanx Fracture

Diego Alejandro Nunez[*a], Andres Bernal[a], Mauricio Felipe Mauledoux[b], Oscar F. Aviles[b]

[a]Grupo de Investigación en Ingeniería Biomédica. Vicerrectoria de Investigaciones. Universidad Manuela Beltrán. Av. Circunvalar No 60-00, Bogotá, Colombia.
[b]Mechatronic Engineering, Davinci Research Group, Universidad Militar Nueva Granada, Av Calle 100, Bogotá, Colombia.
diego.nunez@docentes.umb.edu.co

The phalanx-biomedical device is studied in a finite element analysis software and simulations varying load were carried out. The aim of the research is to describe the mechanical behavior of a device to repair phalanx fracture made of poly-L-lactide acid. Tensile and relaxation behaviors of the polymer are determined and a rheological model is developed as well as the fracture phalanx joined with a polymer device using computer-aided design software. Results indicate that the rheological model with two Neo-Hookean networks in a parallel distribution generates a fit of 98 %. After the analysis of different loads, there is a major relation between time, slope and permissible load time. The stress associated with change in geometry owing to the holes in the bone is the principle cause of biomedical device failure. The Von Mises stresses were more than 3.2 times yield stress for all simulations except with the lowest load. As conclusion, the use of finite element analysis avoids destructive tests and reduces resources. In addition, a mathematical description of the mechanical behavior of the poly-L-lactide acid is accomplished by using a Parallel Network Model.

1. Introduction

Hand fractures are among the most common skeletal injuries and one of the hardest to handle. This phenomenon depends on variables such as age, fracture configuration, location, type of fixation, and excessive digital immobilization (Duncan et al. 1993). Invasive or non-invasive procedures are commonly used to stabilize displaced bone fractures and there are many fixation methods and implants reported (Dumont et al. 2007). Formerly, those implants were made of metals although they produced many complications (Avilés et al. 2016). In order to minimize the complexities, bio-absorbable devices made of biopolymers have been developed for their ability to be adjustable to specific requirements such as micro-structural array, no toxicity, no need for additional surgery to remove the implant, and appropriate mechanical response (Bergström & Hayman 2016). In this context polylactide (PLA) can be mentioned and it exists as two stereoisomers: poly-D-lactide acid (PDLA), poly-L-lactide acid (PLLA), and a racemic mixture named PDLLA (Onuma & Serruys 2011). Challenges with PLLA devices used in orthopedic applications are related to its type, location into the body, and the associated mechanical requirements. It has been demonstrated that PLLA exhibits premature failure at stress magnitudes that are significantly lower than the ultimate tensile and yield strength of the material, due to its viscoplastic flow causing creep rupture or fatigue failure (Bergström & Hayman 2016). Hence, the device is likely to fail before expected, if the material undergoes in vivo degradation. Therefore, material behavior prediction based on non-viscoplastic model, deformation, time and failure model is necessary. To predict the mechanical behavior, it is necessary to use a mathematical model, which describes the relation between stress, strain, temperature, and strain rate. The non-linear mechanical response of PLLA has an influence on the device performance; however, there is an insufficient information about mathematical models capable to predict material behavior under physiological conditions (Avilés et al. 2016). This paper is focused on the mechanical performance of a phalanx fracture repairing device consisting of PLLA based on material tensile behavior and Parallel Network Model (PNM). Furthermore, the study of convergence of mesh density and the analysis of critical zone of repair are presented.

2. Materials and methods

2.1 Polymer features

PLLA stereo-regular homo-polymer was provided by PURAC Biochem (Gorinchem, The Netherlands). The initial inherent viscosity of material was 8.28 dL/g, mean crystallinity of 37 %, mean glass transition of 63 °C, mean melting temperature 175 °C, Young's modulus between 500 MPa and 2 GPa and elongation to failure from 20 % to 150 %. Degradation *in-vivo* environments occurs in two years approximately.

2.2 Mechanical behavior of PLLA

Tension properties of the material were determined following standard ASTM D638-10. PLLA specimens were tested under different conditions. The first test was a uniaxial tensile test set with 0.05/s strain rate (Figure 1). The second test was set with 0.001/s strain rate (Figure 1). In the third test, specimen suffered a relaxing behavior as shown in Figure 1 and 2. The next step was to determine the implementation of the mathematical model. Three simulations to select the best rheological model were analyzed as is depicted in Figure 3. The first model was based on the stress parameter considering the Neo-Hookean hyperelastic behavior (Eq (1)) represented in Figure 3a. Neo-Hookean hyperelastic behavior considered the force applied on the solid as an independent factor, and both shear modulus and bulk modulus as dependent factors. Dependent factors values were unknown. The second simulation (Figure 3b) considered a Neo Hookean hyperelastic behavior and a power flow with double exponential yield evolution (Eq (2)). Additionally, simulation took into account the exponential yield evolution and considered two evolution factors and two transition strains, each of them unknown. The third simulation (Figure 3c) was carried out with two networks in parallel. The first one described a Neo Hookean hyperlelastic behavior and the second network depicted the same Neo Hookean hyperelastic behavior with same unknown values about shear modulus and bulk modulus. The second network contains a flow component as well, which was represented as a power flow with double exponential yield evolution (Eq (2)). This flow component depends on pressure, temperature and flow evolution (Eq (3)).

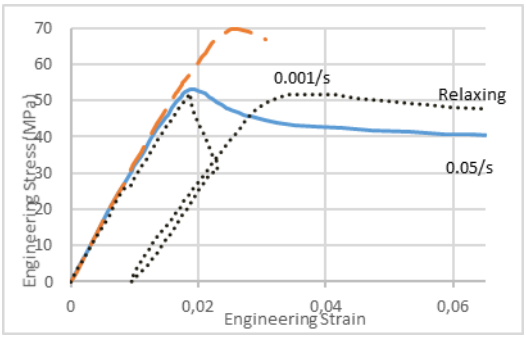

Figure 1. Experimental tests varying strain rate and relaxing behavior.

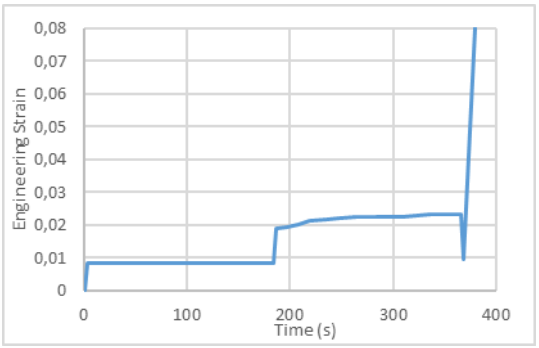

Figure 2. Relaxing strain time behavior.

2.3 Obtaining of parameters of constitutive equation

The material parameters were obtained using the Nelder Mead Simplex algorithm method. Once the optimization algorithm was finished, the rheological configuration with the lowest root mean square error (RMSE) was chosen. The RMSE was used as the objective function. The material parameters were obtained following two steps. The first step established the experimental data (Figure 1 and 2). Second, the material model was selected including hypereslastic behaviors and flow features. As a result, the third configuration generated the best fit regarding to experimental behavior.

$$\sigma = \frac{\mu}{|F|} dev\left(|F|^{-\frac{2}{3}} F F^{T}\right) + \kappa(|F| - 1)I \quad (1)$$

Where:

σ:	Cauchy stress.	κ:	Bulk modulus.	F:	Force.
μ:	Shear Modulus.	FT:	Force transpose.	I:	Identical Matrix

$$f_r = \left(\frac{\tau}{R_\tau f_p f_T f_E}\right)^m \quad (2)$$

Where:

fr:	Flow rate.	*Rτ:*	Shear flow resistance.
τ:	Shear stress.	*m:*	Shear flow exponent.

f_p: Pressure dependence factor =1.

f_T: Temperature dependence factor=1.

f_E: Flow evolution factor Eq (3).

Internal body conditions do not have considerable variation respect to environmental pressure and temperature. (Kasper et al., 2016)

$$f_E = \frac{1}{2}\left[\left(A + (1-A)e^{\frac{-\varepsilon_M}{E_1}}\right) + \left(B + (1-B)e^{\frac{-\varepsilon_M}{E_2}}\right)\right] \quad (3)$$

Where:

A: Final value of flow evolution factor for exponential 1.

ε_M: Effective Mises plastic strain.

E_1: Characteristic transition strain for exponential 1.

B: Final value of flow evolution factor for exponential 2.

E_2: Characteristic transition strain for exponential 2.

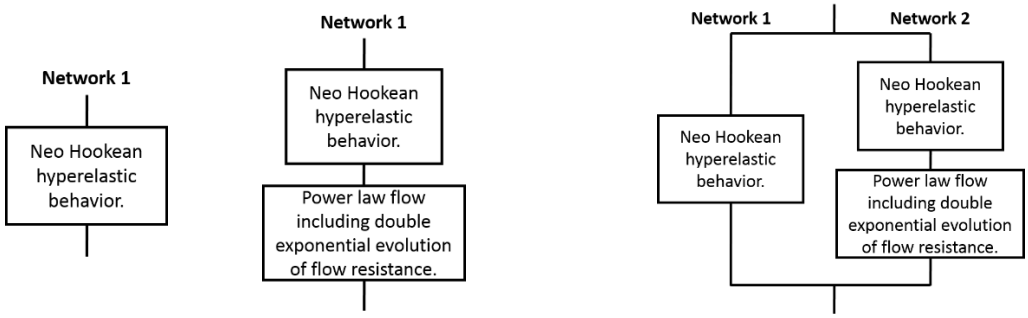

Figure 3. Rheological representation of Parallel Network model. (a) First simulation. (b) Second simulation. (c) Third simulation.

2.4 Mechanical behavior of phalanx bone and biomedical device

The main objective of the research was to study the tensile behavior of a computer-aided model of a fractured phalanx joined by a medical device and two pins, all of them made of PLLA (Figure 4). The phalanx model developed by Holzbaur *et al*. (Holzbaur et al. 2005) on the OpenSim platform (Delp et al. 2007) was used. The biomedical device was a rectangular piece of 16 mm length, 4 mm width and 1 mm thickness, and rounded edges with 2mm radius. It had two holes of diameter 1.6 mm and distance between center was 12 mm. Pins had 1.6 mm diameter and 4.5 mm length. The head had 9.4 mm diameter and 1.2 mm length. Both, the phalanx and the biomedical device were modeled with Autodesk Inventor software. After modeling, the assembly was exported to Ansys® Workbench software and the finite element analysis was carried out.

Figure 4. Phalanx joins with PLLA device. (a) Fixed support. (b) Force applied in FEA.

Table 1. Load configurations. Each load applied during certain time generated a slope.

	Load time (s)	0.20	1.00	2.00	4.00	8.00
Load (N)						
2.00	Slope	10.00	2.00	1.00	0.50	0.25
5.00	(N/s)	25.00	5.00	2.50	1.25	0.62
10.00		50.00	10.00	5.00	2.50	1.25
20.00		100.00	20.00	10.00	5.00	2.50

At the end of a half phalanx, the boundary condition was determined as fixed (Figure 4a); the boundary condition simulated the join between the phalanx and metacarpus. Next, an axial force was located at the end of the other half phalanx (Figure 4b). The applied loads presented ramp behaviors are depicted in Table 1.
The phalanx modulus was 16 GPa, with a Poisson´s ratio of 0.3, tensile yield strength of 80 MPa, and compressive yield strength of 117 MPa (Enderle & Bronzino 2011). Once the parameters were obtained, mechanical performance of PLLA was determined. Some studies have demonstrated the influence of the mesh density on the response of the finite element analysis (Liu & Glass 2013). Hence, the appropriate element size was determined. To obtain accurate response, the simulation with a load of 5 N, time 1 s and a slope of 5 N/s was implemented using 5 different size elements: 0.18 mm, 0.35 mm, 0.53 mm, 0.61 mm, and 0.7 mm. The highest element size was chosen, showing a convergence behavior of less than 1 %; this mesh density was also used for the rest of the simulations because of its higher computational efficiency. The time that phalanx and device could support loads without presenting plastic deformation was studied. According to each load conditions (Table 1), there was a time when the Von Mises stress of the assembly was equal to yield stress. The maximum time period in which the assembly bears the load was called Maximum Load Time, and the period of time during which the load was applied was called Load Time (Figure 5).

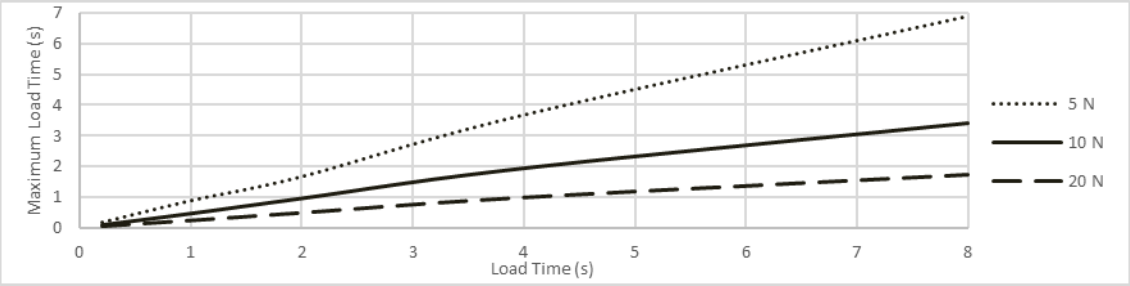

Figure 5. Relation between load time and maximum time that the assembly bear without plastic strain.

3. Results and discussion

The RMSE served to evaluate the difference between the observed and the predicted value for each of the three rheological models performed were 0.520, 0.040 and 0.020 respectively. Once the optimization process was carried, the third simulation parameters of Network 1 and Network 2 which generated the best fit were defined. The obtained parameters of Network 1 (**Errore. L'origine riferimento non è stata trovata.**c), described as a Neo Hookean hyperelastic behavior were: μ= 60.251 MPa and κ =5191.040 MPa. The parameter values of Network 2 were defined as presented in Table 2.

Table 2. Obtained Parameters of Network 2.

μ (MPa)	κ (MPa)	Rτ (MPa)	m -	fp -	f_T -	A -	E1 -	B -	E2 -
1009.470	5920.130	69.316	13.825	1.000	1.000	0.016	0.032	-0.016	9.580

Where: - = dimensionless.

Once the parameters of two networks were defined, the mathematical model was compared against experimental data. Figure 6 shows the experimental and predicted behaviors. Phalanx and device were analyzed using the same element size of 0.53 mm, which was the largest element size that showed a variation convergence behavior of less than 1 % (Figure 7). This element size was chosen in order to perform the rest of the simulations. All simulations demonstrated that maximum stresses were around the holes. Figure 8 shows Von Mises stress (383 MPa aprox.) around holes for 10 N load and 5 N/s slope. Von Mises stress close to holes was 4.8 times greater than yield stress of bone. The same tendency had 5 N, 10 N and 20 N loads when the zones around the holes were analyzed and Von Mises-yield stress ratios were between 3.2 and 5.6. These results agreed with literature (Trojan 1986), which suggested that defects on structures such as holes, geometry changes, and cracks incremented stress and generate failure. Nevertheless, the device's performance in all simulations was below yield stress. Figure 9 depicted the Von Mises stress of device when load was 20 N and the slope equal to 100 N/s. Figure 5 shows the relation between the load time and the time in which the device can hold load without exceeding the elastic limit of each material. The assembly did not depict a yield behavior under a load of 2 N. After comparing among three possible rheological configurations, the third configuration demonstrated the best fit (Figure 3c). The first configuration only considered hyperelasticity behavior of the polymer, and as a result, the mechanical behavior did not respond to flow and

the molecular bonds did not fail. The second configuration included flow responses that evidenced a good fit related to relaxation behavior. The Neo-Hookean hyperelasticity with a power law flow described accurately covalent bond strength and flow relation on mechanical performance of material. These results are in concordance with the theory. The viscoelastic flow response is non-linear, since otherwise, the model framework will be the same as a linear viscoelasticity which is insufficient for capturing the general response of the polymer (Bergström 2015). A third viscoplastic configuration was proposed in order to establish the influence of intermolecular forces on material behavior; as a consequence, the RMSE decreased. Based on these results, the first network of the third model exposed the hyperelasticy related with intermolecular forces and the second network of the third model, described the intramolecular resistance and its performance taking into account the flow. This representation based on the decomposition of the total stress into an elastic and history dependent component is in a good agreement with prior studies (Bakker 2012). The polymeric material model supported in the PNM determined that the shear modulus related to intramolecular flow resistance is almost 17 times higher than the shear stress related to intermolecular resistance. It demonstrated that Van der Waals forces are not enough to maintain the polymeric chains joined under a load, and the main strength is based on the strength of the covalent bonds (Bergström 2015). Since element size has a direct influence in the response and its accuracy, a relation between mesh density and convergence was carried out. This comparison demonstrated that a mesh density with element sizes equals to 0.53 mm converged equally as more refined mesh densities. Making a comparison between 0.53 mm and 0.18 mm element sizes, responses differ in less than 1 %, although bigger mesh density consumed less computer resources and computing time (Liu & Glass 2013).

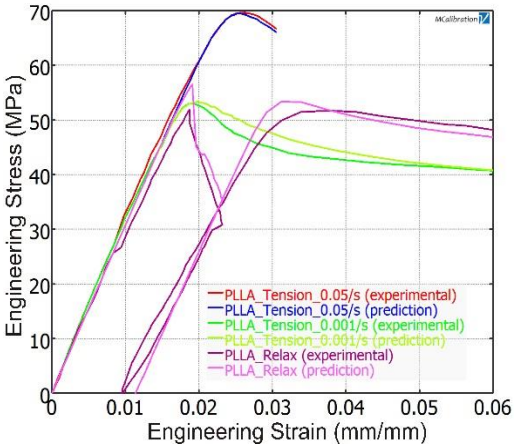

Figure 6. PLLA Tensile behavior varying strain rate and relaxation. Comparison between experimental data and prediction data.

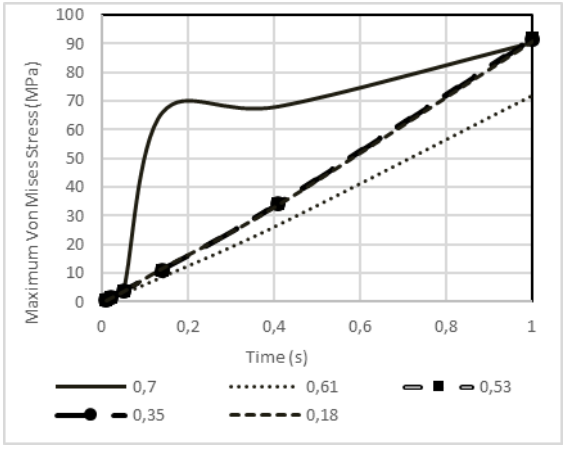

Figure 7. Influence of size element on Maximum Von Mises Stress.

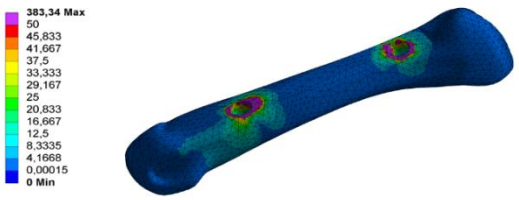

Figure 8. Equivalent Von Mises stress in phalanx.

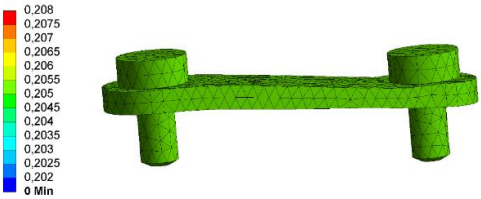

Figure 9. Equivalent Von Mises stress of biomedical device.

Figure *6* demonstrates that prediction of the mechanical behavior can accurately determine the ultimate stress. Furthermore, the elastic modulus was correctly predicted as well as the fracture stress defined. Stress between ultimate stress and stress at 0.048 mm/mm at tensile test with strain rate of 0.001 /s depicted a gap. The difference between experimental and predicted behavior is due to the flow evolution factor, which related the flow response with the plastic strain. Relaxation behavior showed this difference better at stress related with 0.031 mm/mm (Bergstrom 2012). The relation between the strength and the useful stress depend only upon the slope of the load; it depended on the combination between the slope and the load time instead. Although some loads have equal slopes, the bearing of assembly was lesser when the load was applied during a longer period of time as a result of the intramolecular strength (Van Krevelen & Te Nijenhuis 2009).
This research evidenced the relevance of the stress concentrations in bone when the fixed elements were used. Figure 8 showed that higher stresses are located around the holes whereas the extremes of the phalanx

do not bear the load. Although the initial focus of this work was studying the strength of the PLLA device, once the simulation data were analyzed the device bore lower stress than yield stress without great variations (Figure 9). Hence, stress concentration because of holes of bones is the main cause of the assembly failure.

4. Conclusions

The Parallel Network Model with two parallel networks accurately described intermolecular and intramolecular incidence on mechanical behavior of PLLA. The viscoplastic model includes the inference of strain rate, temperature, relaxation response, hyperelasticity and flow response. Furthermore, flow evolution factor presents an influence on flow response at plastic strains. The convergence of simulation response was related to the mesh density factor. In addition, internal conditions of the hand do not have relevant effects on mechanical behavior of biomedical device compared to its behavior in environmental conditions. Strength of the device is related to the load, the load rate, and the time. Once the analysis was accomplished, in order to use bio-absorbable plate with pins to repair fracture phalanx, it is necessary focusing in some aspects. The use of this kind of array has to take into account stress concentration due to fixing holes in the bones. The bio-absorbable material has adequate strength to bear tensional loads related to daily activities. Future analysis should include degradation, anisotropic behavior of materials and studies about torsional and compressional responses.

References

Avilés, O. F. S., Mauledoux, M. F. M., Rubiano, O. G. M., Ramirez, H. F. G. and Dutra, M. S. (2016) 'FEA of Bioabsorbable Material to Repair Hand Fractures', *Applied Mechanics and Materials*, 823, pp. 173–178. doi: 10.4028/www.scientific.net/AMM.823.173.

Bakker, K. (2012) 'Water Security: Research Challenges and Opportunities', *Science*, 337(6097), pp. 914–915. doi: 10.1126/science.1226337.

Bergström, J. (2015) 'Viscoplasticity Models', in Bergström, J. (ed.) *Mechanics of Solid Polymers*. Elsevier, pp. 371–436. doi: 10.1016/B978-0-323-31150-2.00008-X.

Bergstrom, J. S. (2012) 'PolyUMod--A Library of Advanced User Materials', *Veryst Engineering, LLC, Needham, Mass, USA*.

Bergström, J. S. and Hayman, D. (2016) 'An Overview of Mechanical Properties and Material Modeling of Polylactide (PLA) for Medical Applications', *Annals of Biomedical Engineering*. Springer, 44(2), pp. 330–340. doi: 10.1007/s10439-015-1455-8.

Delp, S. L., Anderson, F. C., Arnold, A. S., Loan, P., Habib, A., John, C. T., Guendelman, E. and Thelen, D. G. (2007) 'OpenSim: Open-Source Software to Create and Analyze Dynamic Simulations of Movement', *IEEE Transactions on Biomedical Engineering*. IEEE, 54(11), pp. 1940–1950. doi: 10.1109/TBME.2007.901024.

Dumont, C., Fuchs, M., Burchhardt, H., Appelt, D., Bohr, S. and Stürmer, K. M. (2007) 'Clinical Results of Absorbable Plates for Displaced Metacarpal Fractures', *Journal of Hand Surgery*, 32(4), pp. 491–496. doi: 10.1016/j.jhsa.2007.02.005.

Enderle, J. and Bronzino, J. (2011) *Introduction to Biomedical Engineering*. Elsevier Science (Biomedical Engineering).

Holzbaur, K. R. S., Murray, W. M. and Delp, S. L. (2005) 'A Model of the Upper Extremity for Simulating Musculoskeletal Surgery and Analyzing Neuromuscular Control', *Annals of Biomedical Engineering*. Springer, 33(6), pp. 829–840. doi: 10.1007/s10439-005-3320-7.

Hughes, T. B. (2006) 'Bioabsorbable Implants in the Treatment of Hand Fractures', *Clinical Orthopaedics and Related Research*. LWW, PAP, pp. 169–174. doi: 10.1097/01.blo.0000205884.81328.cc.

Kasper, D. L., Fauci, A. S., Hauser, S., Longo, D., Jameson, J. L. and Loscalzo, J. (2016) *Harrisons Manual of Medicine, 19th Edition*. McGraw-Hill Education.

Van Krevelen, D. W. and Te Nijenhuis, K. (2009) 'Mechanical Properties of Solid Polymers', in Krevelen, D. W. Van, By, R., and Nijenhuis, K. Te (eds) *Properties of Polymers*. Fourth Edi. Amsterdam: Elsevier, pp. 383–503. doi: 10.1016/B978-0-08-054819-7.00013-3.

Liu, Y. and Glass, G. (2013) 'Effects of Mesh Density on Finite Element Analysis', in. doi: 10.4271/2013-01-1375.

Onuma, Y. and Serruys, P. W. (2011) 'Bioresorbable Scaffold: The Advent of a New Era in Percutaneous Coronary and Peripheral Revascularization?', *Circulation*. Am Heart Assoc, 123(7), pp. 779–797.